PROCESS DRIVEN ENERGY MANAGEMENT FOR EFFICIENT GALLEY OPERATIONS

L. Yu , R. God
Hamburg University of Technology, Institute of Aircraft Cabin Systems, Hein-Saß-Weg 22, 21129 Hamburg, Germany

Abstract

A key objective in the design of new aircraft systems is the continuous improvement of overall aircraft efficiency. To achieve this, multiple perspectives, *e.g.*, inside the aircraft galley, are considered, such as process efficiency, weight efficiency, energy efficiency, operational efficiency, etc. Traditionally, aircraft manufacturers apply a top-down approach of electrical system design, where fixed power budgets are allocated to subsystems based on "worst-case" peak loads in specific flight phases. This this sum of nominal loads can lead to overfitted electrical distribution networks. Therefore, this paper presents a bottom-up design and the implementation of a thermal and electrical energy management system for galley operations. An advanced galley energy management approach based on thermal and electrical energy consumption and a decentralized active control within the galley is used. The proposed intelligent control strategy dynamically adjusts heating, cooling and galley inserts operation to maintain optimal power consumption for thermal systems and increase electrical energy efficiency without negative impact on service quality. Results demonstrate significant reduction of the peak in electrical energy consumption and make reductions of weight from electrical power supply system possible due to lower requirements of the maximum amplitude of power and current. This approach offers a potential solution to increasing efficiency in the galley, adapting the workflow of cabin crew, and contributing to future design of aircraft galleys.

Keywords

aircraft cabin, galley inserts (GAINs), thermal modeling, efficient operation, process driven load management

1. INTRODUCTION

Efficiency is one of the key objectives in aircraft design, while the aviation industry is facing unprecedented pressure to improve sustainability and reduce environmental footprint and carbon emissions. Significant research focuses on aerodynamic design, advanced propulsion and lightweight materials, while the optimization of aircraft cabin systems, with a focus on the galleys, presents a high potential of energy savings and better electrical efficiency. In fact, a commercial aircraft galley can have a total power demand of up to 120 kVA in an Airbus A350, making it the largest non-propulsive consumer of electrical energy onboard [1]. Because of this substantial power demand, the galley holds a large potential for electrical energy system optimization.

During long-haul flights, galley equipment is operated in complex and overlapped duty cycles. Galley inserts (GAINs), such as ovens, water boilers and coffee makers, impose significant, simultaneous thermal and electrical loads. Traditionally, aircraft manufacturers apply a top-down approach of electrical system design, where fixed power budgets are allocated to subsystems based on “worst-case” peak loads. This approach often leads to an overfitted electrical distribution network, sub-optimal energy management, and, increasing fuel consumption. While existing literature widely addresses optimization at the top-level aircraft power distribution tier, and, other papers design and develop the electrical energy system considering the whole aircraft [2] and the environmental control system [1], there is still a lack for optimization and improvement of electrical energy consumption in the galleys. Schlabe and Lienig [3] reviewed extensive energy management methods for aircraft electrical networks, exploring overall load allocation and macro-level load-shedding to safeguard generators against catastrophic overload already in 2012. Conventional galley configurations typically consider the maximum nominal power as the summation of all installed GAINs, while the operation has fixed-priority and influences the workload of cabin crew. To achieve efficient galley operations, a dynamic understanding of these interactions of GAINs and catering operations onboard is needed.

Previous studies often treated galley power consumption as uniform and static loads, completely overlooking the transient thermal behaviors and electrical power load profiles. This paper steps into this gap by developing comprehensive thermal and electrical models for the primary energy consumers in an aircraft galley: the oven, the water heater, and the coffee maker. By characterizing their transient power demands and thermal efficiencies, this research provides a reliable simulation model. Simulation data are in line with real measurement data from a GAIN test-setup [4]. Based on these models, we propose and evaluate a priority-based control algorithm to intelligently manage load distribution, eliminate peak power spikes without compromising operations and passenger comfort. The subsequent sections of this article are structured as follows. Section 2 introduces the thermal and electrical models of GAINs considered in aircraft as heavy loads. Section 3 describes the intelligent control algorithm. Section 4 presents the results of the entire simulation. Section 5 discusses the potential of system load reduction. Section 6 summarizes the results and identifies future work.

CC BY 4.0

doi: 10.25967/680018

2. MODELING

Main method in this paper is to model and simulate the thermal and electrical behavior of GAINs with high power load, e.g., ovens, water heaters and coffee makers. Lumped parameter models are successfully used in other studies, e.g., thermally multi layered buildings [5] and thermal modelling of domestic appliances [6]. As our main purpose is to elaborate electrical load profiles, we apply this network similarity to simplify the thermal behavior of GAINs by using the analogy of thermal parameters with electrical parameters. We assume, electrical current is analog to heat transfer, voltage to temperature, capacitor to thermal mass or specific heat capacity, and ohmic resistance to thermal resistance. This paper investigates temperature response given by differential equations for the considered circuit model.

2.1. Oven

An oven under consideration is mainly used for preparing hot meals for passengers. As a thermal system, electric ovens cannot be easily modeled because the temperature responses and thermal behavior are not directly determined by the heating process. A much wider variety of technical design and parameters, such as the heating element, the oven cavity, surface to the environment etc., must be considered as elements of the whole process. However, our purpose is to build up a plausible thermal model to determine the electrical power consumption pattern.

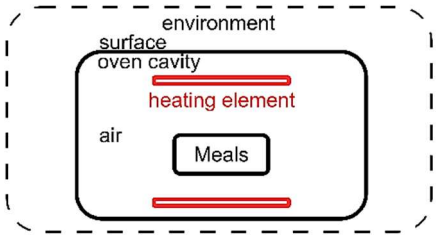


FIG 1. sketch of a thermal oven system

The thermal model can be simplified as shown in Figure 1. The model includes four temperature variables, heating element temperature, oven cavity air temperature, oven surface temperature and meal temperature. We assume, the environment temperature T_{air} is constant at 20 °C due to cabin environmental control system.

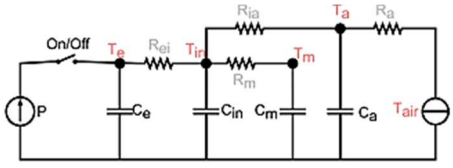


FIG 2. lumped parameter model circuit for an oven

The thermal system model of the circuit in Figure 2 is characterized by differential equations written as state space equations below:

(1) $$\dot{x}(t) = Ax(t) + Bu(t)$$
$$y(t) = Cx(t) + Du(t)$$

(2) $$x(t) = \begin{bmatrix} T_e \\ T_{in} \\ T_m \\ T_a \end{bmatrix}, u(t) = \begin{bmatrix} P \\ T_{air} \end{bmatrix}$$

(3) $$\dot{x}(t) = \begin{bmatrix} \frac{dT_e}{dt} \\ \frac{dT_{in}}{dt} \\ \frac{dT_m}{dt} \\ \frac{dT_a}{dt} \end{bmatrix} and, y(t) = T_{in}$$

(4) $$A = \begin{bmatrix} -\frac{1}{R_{ei}C_e} & \frac{1}{R_{ei}C_e} & 0 & 0 \\ \frac{1}{R_{ei}C_{in}} & -(\frac{1}{R_{ei}C_{in}} + \frac{1}{R_{im}C_{in}} + \frac{1}{R_{ia}C_{in}}) & \frac{1}{R_{im}C_{in}} & \frac{1}{R_{ia}C_{in}} \\ 0 & \frac{1}{R_{im}C_m} & -\frac{1}{R_{im}C_{in}} & 0 \\ 0 & \frac{1}{R_{ia}C_a} & 0 & -(\frac{1}{R_{ia}C_a} + \frac{1}{R_aC_a}) \end{bmatrix}$$

(5) $$B = \begin{bmatrix} \frac{1}{C_e} & 0 \\ 0 & 0 \\ 0 & 0 \\ 0 & \frac{C_a}{R_a} \end{bmatrix}, C = [0 \quad 0 \quad 1 \quad 0]$$

Where, C_e, C_{in}, C_a and C_m are the specific heat capacity of heating element, air inside oven cavity, oven surface and meals (J/°C). R_{ei}, R_{ia}, R_a and R_m are the thermal resistance between heating element and oven cavity, between oven cavity and oven surface, between oven surface and environment and between oven cavity and meals (W/°C). T_e, T_{in}, T_a and T_m are the temperature of heating element, air inside oven cavity, oven surface and meals (°C).

2.2. Water Heater

The Water Heater under consideration in this study is primarily used to supply hot water for passengers. The heater consists of a storage tank where water is heated by an electric heating element regulated by an on/off thermostat. Additionally, the tank features an inlet for incoming cold water and an outlet pipe for hot water delivery. While existing literature [7] presents a water heater model in terms of energy flow as done in [6], this study describes a water heater model specifically designed to simulate electric power consumption as a function of the heater's on/off states.

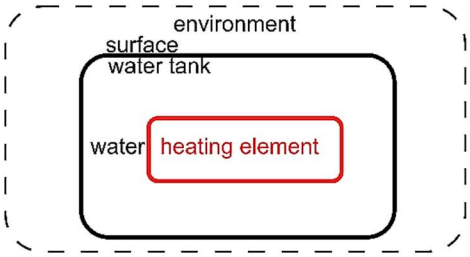


FIG 3. sketch of a thermal water heater system

To determine the internal tank water temperature, the system was modeled using a simple lumped thermal circuit, assuming a uniform temperature distribution throughout the water volume.

CC BY 4.0

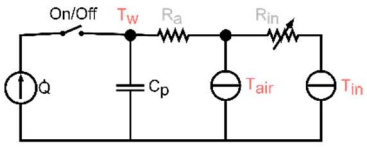


FIG 4. lumped parameter circuit for water heater

The thermal system model of the circuit in Figure 3 can be written as differential equation as below:

$$\rho C_p V \frac{dT_w}{d_t} = UA(T_w - T_{air}) + \rho C_p(T_w - T_{in}) + \dot{Q} \quad (6)$$

Where C_p is the water specific heat capacity (4.184 J/(g·K)), ρ is the density of water (0.998 g/cm3), V is the volume of water tank, T_w, T_{in}, and T_{air} are the Temperature of water inside tank (°C), temperature of water entering the tank (°C) and the constant environment temperature 20 °C, U is the thermal transmittance of tank, A is the surface area of tank, $\dot{Q}$ is the energy input (W).

2.3. Coffee maker

The coffee machine operates without much difference compared to a water heater. The water supply is mainly used for brew coffee, and with each brewing process, water is only supplied once. The thermal model can be simplified into only three nodes, heating element, water in tank and environment.

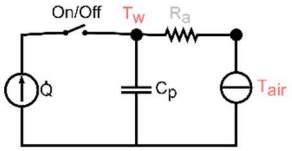


FIG 5. lumped parameter circuit for coffee maker

$$\rho C_p V \frac{dT_w}{d_t} = UA(T_w - T_{air}) + \dot{Q} \quad (7)$$

Where C_p is the water specific heat capacity (4.184 J/(g·K)), ρ is the density of water (0.998 g/cm3), V is the volume of water tank, T_w and T_{air} are the Temperature of water insides tank (°C) and the constant environment temperature 20 °C, U is the thermal transmittance of tank, A is the surface area of tank, $\dot{Q}$ is the energy input (W).

2.4. Catering process onboard

To optimize the electrical energy consumption and power sharing within the galley, it is necessary to understand the catering process onboard. This paper considers Boeing 777-300ER aircraft from Turkish Airlines [8] as a reference flight to determine the service process. The flight can carry max. 349 passengers with 300 economy and 49 business class seats. Four galleys are installed in total, comprising three economy and one business class galley. The latter one and respective passengers are not considered, because in business class the catering process is more agile and not that standardized than in economy class. These procedural conditions lead already to a flatter power consumption. Thus, we consider the catering process with 300 passengers and three galleys in economy class. We assume, the galleys have identical configurations and passengers are assigned evenly across three galleys, i.e., the catering process model can be simplified into one galley for 100 passengers. In our case a standard galley monument consists of three ovens, one water heater and one coffee maker. During the meal service, hot beverages will be served firstly, followed by warm meals, and a final round of drinks.

3. CONTROL ALGORITHM

As a participant in the aircraft electrical power system, the galley represents one of the largest non-essential peak loads. Simultaneous operation of high-power thermal loads — such as steam ovens, water heaters, coffee makers, and refrigeration units — can drive instantaneous power consumption to 100% of total installed capacity, however, lasting only for a very short period of time. This leads to an unnecessary oversizing of electrical power generators and electrical wiring installation.

To alleviate peak demand without sacrificing user functionality or violating thermal constrains, we present a priority-based load control algorithm with adaptive weight. The primary goal of the energy management system is to maintain aggregated electrical power consumption below a pre-configured cap of $P_{total} \leq \eta P_{installed}$. We aim to achieve a 40% reduction in peak power demand, corresponding $\eta \leq 0.60$.

3.1. Priority-based control

Let the galley system consist of N discrete electrical loads $i \in \{1,2,\dots,N\}$. Each load has a nominal rated power P_i and a standby power $P_{s,i}$. The operational state of load i at discrete time step t is denoted by $s_i(t)$, where $s_i(t) \in \{0,1\}$ represents discrete state allocation of $s_i(t) = 0$ for OFF, $s_i(t) = 1$ for ON.

The instantaneous total power consumption $P_{total}(t)$ must satisfy the global threshold constraint:

$$P_{total}(t) = \sum_{i=1}^{N} s_i(t) \cdot P_i \leq \eta P_{installed}, \forall t \quad (8)$$

For thermostatically controlled GAINs (e.g., ovens, water heaters, coffee makers) reducing $s_i(t)$ alters the internal thermal equilibrium. The internal temperature $T_i(t)$ of GAIN i at time step t is modeled in previous chapters. To preserve food safety regulations of Hazard Analysis and Critical Control Point (HACCP standards) and culinary quality, $T_i(t)$ must remain bounded within explicit lower and upper operational safety thresholds [9]:

$$T_{i,min} \leq T_i(t) \leq T_{i,max} \quad (9)$$

If $T_i(t)$ approaches $T_{i,min}$ for heating loads or $T_{i,max}$ for cooling loads, the control algorithm must prohibit further load shedding ($s_i(t) \to 1$) by shut down other GAINs immediately.

The control optimization problem is expressed as a constrained dynamic utility maximization problem evaluated at each discrete time step t. The overarching objective is to allocate power across all connected GAINs in a manner that maximizes system-wide operational utility while adhering to the global peak power limit and physical state constraints.

In the foundational formulation of the algorithm, each GAIN i is assigned a static, constant priority weight PR_i based on its default functional criticality. Regarding this baseline, the optimization problem is expressed as:

CC BY 4.0

(10) $$\max_{s_i(t)} \sum_{i=1}^{N} PR_i \cdot s_i(t) \cdot P_i$$

This static priority framework ensures critical safety, and preservation loads take precedence over secondary loads, while static weights alone can lead to prolonged load shedding and "starvation" of low-priority equipment during extended service periods. To overcome these operational limitations, section 3.2 introduces the dynamic adaptive weight mechanisms – incorporating real-time thermal drift and deferral wait times – which dynamically modifies PR_i into a time-varying priority index $PR_i(t)$.

3.2. Adaptive weight

In traditional energy management systems, appliances are assigned fixed, static priority levels based only on functional importance. While effective for short peak transients, static priority schemes implicate two fundamental operational weaknesses in galley systems. 1. Equipment starvation: Low-priority appliances can be continuously shed during sustained high-demand operational windows (*e.g.*, first onboard meal service preparation). Prolonged power permission prevents these GAINs from completing whole basic catering cycles and degrading cabin service quality. 2. Thermal constraints violations: medium- and high-priority thermal GAINs work dynamically. Under static weighting, a medium-priority oven that has significantly fallen below its target temperature carries the same priority as an oven operating near setpoint. Static weighting fails to reflect instantaneous thermal urgency.

To eliminate starvation while maintaining total aggregated power below the threshold $P_{total} \leq \eta P_{installed}$, static priority factors PR_i are transformed into a dynamic, time-varying priority index $PR_i(t)$. The instantaneous priority index $PR_i(t)$ for GAIN i at discrete time step t is defined as a multi-variable additive dynamic function:

(11) $$PR_i(t) = \omega_{base,i} + \omega_{temp,i}(t) + \omega_{wait,i}(t)$$

where: $\omega_{base,i}$ is the static base criticality weight reflecting inherent safety and operational tier, $\omega_{temp,i}(t)$ is the time-varying thermal weight based on deviation from pre-set temperature, $\omega_{wait,i}(t)$ is the time varying starvation prevention weight based on continuous shedding duration.

The static base weight $\omega_{base,i}$ establishes the baseline hierarchy when all GAINs operate in steady-state equilibrium. GAINs are partitioned into three groups: group 1 with high priority / health and safety ($\omega_{base,i} \in [0.8, 1]$): remote air chiller, oven systems required to prevent food spoilages and maintain international HACCP health compliance [9]. Group 2 with medium priority / service production ($\omega_{base,i} \in [0.4, 0.7]$): water heaters, coffee makers. Group 3 with low priority / auxiliary operations ($\omega_{base,i} \in [0.1, 0.3]$): trash compactor, plate warmers etc.

For thermal GAINs, priority must be dynamically modified as control temperature $T_i(t)$ drifts further from its target setpoint $T_{target,i}(t)$. The temperature error $e_{T,i}(t)$ is defined considering the thermal operation mode:

(12) $$e_{T,i}(t) = \begin{cases} \max\left(0, T_{target,i}(t) - T_i(t)\right), heating \\ \max\left(0, T_i(t) - T_{target,i}(t)\right), cooling \end{cases}$$

The thermal weight is calculated as a proportional function of normalized thermal error $e_{T,i}(t)$:

(13) $$\omega_{temp,i}(t) = k_{T,i} \cdot \frac{e_{T,i}(t)}{T_{i,max} - T_{i,min}}$$

where $k_{T,i}$ is the scaling coefficient of GAIN i, $T_{i,max}$ and $T_{i,min}$ are the allowed operating temperature limits of GAIN i.

When $T_i(t)$ is within acceptable boundaries around setpoint $T_{target,i}$, $\omega_{temp,i}(t) \rightarrow 0$. As $T_i(t)$ decreases or increases, $\omega_{temp,i}(t)$ increases rapidly, elevating $PR_i(t)$ and forcing the energy management system to restore power before temperature violations occur.

To guarantee bounded queue waiting times for low-priority equipment, $\omega_{wait,i}(t)$ accumulates continuously while a GAIN is shed. Let $t_{off,i}(t)$ denote the elapsed duration GAIN i has remained continuously deactivated or throttled below its nominal power draw $s_i(t) < 1$:

(14) $$t_{off,i}(t) = \begin{cases} t_{off,i}(t - \triangle t) + \triangle t, if\ s_i(t) < 1 \\ 0 \qquad\qquad\qquad\qquad if\ s_i(t) = 1 \end{cases}$$

The starvation prevention term is defined as:

(15) $$\omega_{wait,i}(t) = k_{w,i} \cdot t_{off,i}(t)$$

where: $k_{w,i}$ is the starvation weight coefficient of GAIN i.

4. SIMULATION

4.1. Simulation of GAINs

The three model types of GAINs from section 2 are implemented and simulated in MATLAB/Simulink [10]. Simulated oven model described in section 2.1 takes thermal parameters identified by [7] and [11], electrical and physical parameters from [4].

Parameter	C_e (J/°C)	C_{in} (J/°C)	C_a (J/°C)	C_m* (J/°C)
Value	112	3690	4590	32384
Parameter	R_{ei} (°C/W)	R_{ia} (°C/W)	R_a (°C/W)	R_m (°C/W)
value	0.228	0.181	0.102	0.520
Parameter	P_i (W)			
Value	3485			

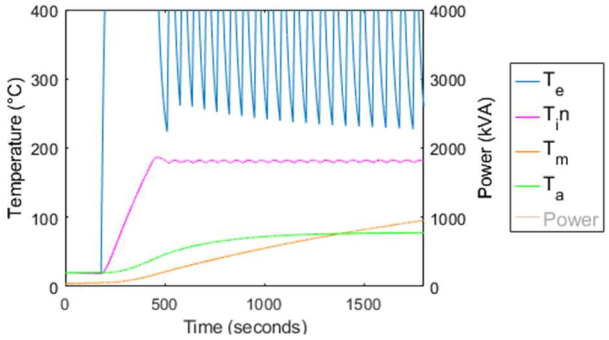
TAB 1. oven parameters

Where, the heat capacity of meals $C_m{}^*$ is varied from [7], while we get the reference data from Safran Cabin Inc. [4]. The oven is capable of heating up to 32 standard aluminum foil containers at the same time, with each container having a capacity of 250 ml and holding $\mathrm{m_i} = 220$ g of mashed potatoes. We adapt the specific heat capacity of mashed potatoes $\mathrm{C_{mp}} = 3.6\,\mathrm{J/(g \cdot K)}$ as an average value between

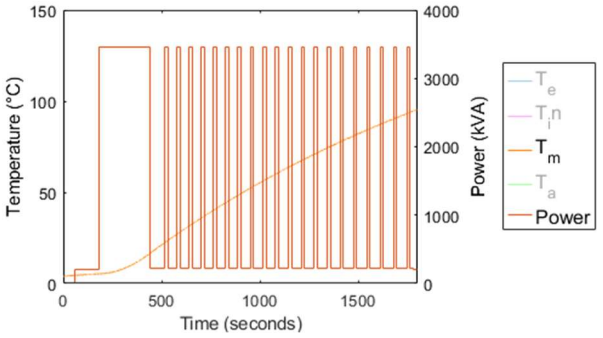
CC BY 4.0

0 °C and 71°C from [13]. We have the total heat capacity of meals as below:

$$C_m{}^* = \sum_{i=1}^{n} m_i C_{mp} = 32384\, J/°C \tag{16}$$



(a)



(b)

FIG 6. (a) oven temperature behavior (b) temperature of meals and power consumption behavior

The simulated thermal behavior and corresponding energy requirements are illustrated in Figure 6. Figure 6 (a) details the comprehensive thermal profile, tracking the transient temperatures of the heating element, oven cavity air, meal target, and external oven chassis. Figure 6 (b) provides a focused analysis on the primary control parameters, specifically comparing the rate of meal temperature elevation against the system's power consumption.

Parameter	ρ (g/cm^3)	C_ρ (J/°C)	U (cm^2)	A (W/m^2K)
Value	0.998	4.19	300	0.4
Parameter	P_i (W)	V (cm^3)		
Value	3600	2400		

TAB 2. water heater parameters

Using the parameters listed in Table 2, the simulation for water heater was conducted over two consecutive heating cycles with an operational interval. Assuming the water heater is activated during the first service cycle, an initial startup phase is required to reach the target setpoint temperature, after which an ON/OFF hysteresis control maintains the temperature above the lower threshold. The resulting thermal dynamics and the corresponding electrical power consumption periods are illustrated in Figure 7.

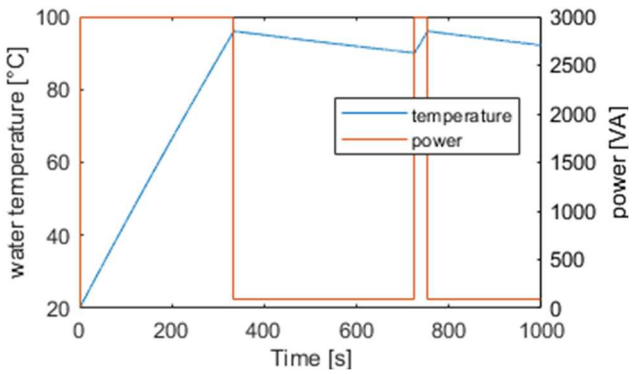


FIG 7. water heater service profile

Parameter	ρ (g/cm^3)	C_ρ (J/°C)	U (cm^2)	A (W/m^2K)
Value	0.998	4.19	260	0.4
Parameter	P_i (W)	V (cm^3)		
Value	2600	1800		

TAB 3. coffee maker parameters

Using the parameters listed in Table 3, the coffee maker simulation was executed across two consecutive brewing cycles. Unlike the water heater system, the coffee maker operates on a single-pass heating process per cycle, eliminating the need for subsequent temperature maintenance. The resulting thermal dynamics and the corresponding electrical power consumption periods are illustrated in Figure 8.

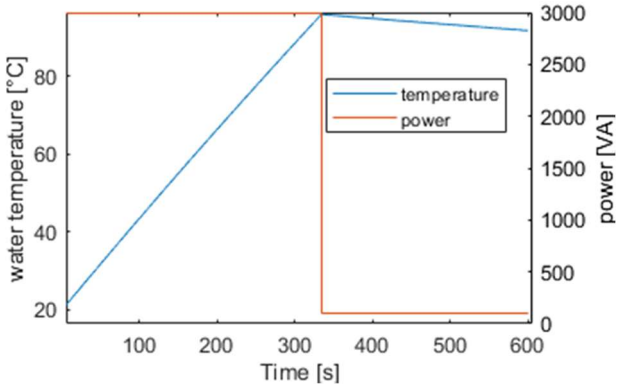


FIG 8. coffee maker service profile

To verify the physical accuracy of the mathematical formulation, the model was validated against experimental hardware measurement profiles provided by Safran Cabin Inc. [4]. The identified thermal parameters and power trajectories demonstrate high plausibility and strong agreement with actual GAIN operating behavior under standard service conditions. These parameters are also in line with the underlying empirical dataset, which cannot be made publicly accessible.

4.2. Integrated System Simulation

To evaluate the performance of the proposed priority-based energy management algorithm under realistic operational conditions, a full-system simulation was implemented in MATLAB/Simulink. The operational scenario is modeled in accordance with the long-haul passenger reference flight described in section 2.4. Each single galley out of three

CC BY 4.0

economy class galleys is dedicated to serve 100 passengers and consists of three ovens, one water heater and one coffee maker. The service schedule follows a standardized three-phase inflight catering profile:

1. Pre-meal hot beverage service: prior to the main course, each passenger receives one hot beverage. We assume for the worst case, passengers order only hot beverages, this volume is distributed equally as 50% hot water (tea/infusions) and 50% fresh brewed coffee. Serving 100 passengers requires a cumulative fluid preparation volume of 50 cups of boiling water, each with a volume of 150 ml, and 50 cups of coffee of the same volume.
2. Main course meal service: following the initial beverage round, 100 hot meals are prepared simultaneously across the three galley ovens.
3. Post-meal hot beverage service: finally, a second hot beverage service round is executed, replicating the previous hot beverage service profile.

Both, the water heater and the coffee maker operate on discrete batch production cycles, where a single operational heating/brewing cycle yields a maximum volume of 12 cups. To fulfill the requirement of 50 cups of hot water and 50 cups of coffee per beverage service phase, the water heater must execute at least 4 service cycles ($4 \times 12 = 48\ cups \approx 50\ cups$) during the pre-meal phase, and another 4 cycles during the post-meal phase. The coffee maker has the same workload. Each convection oven possesses a maximum holding capacity of 32 meals in aluminum shells. To warm up all 100 passenger meals, a cumulative total of 4 oven batch cycles ($4 \times 32\ shells = 128\ shells \geq 100\ meals$) must be executed across the 3 available ovens during the main course preparation window.

The total installed nominal capacity of the galley is:

$$P_{installed} = \sum_{i=1}^{5} P_i = 16.60\ kVA \tag{17}$$

To demonstrate peak load reduction capabilities, the target power limit factor for the simulation setup is designated as $\eta = 0.60$. The control objective for the energy management system is thus set to constrain aggregate demand to a target ceiling of:

$$P_{total} \leq \eta \times P_{installed} = 9.96\ kVA \tag{18}$$

Para.	$\omega_{base,1}$	$\omega_{base,2}$	$\omega_{base,3}$	$\omega_{base,4}$	$\omega_{base,5}$
Value	0.90	0.85	0.80	0.60	0.70
Para.	$k_{T,1}$	$k_{T,2}$	$k_{T,3}$	$k_{T,4}$	$k_{T,5}$
Value	0.02	0.02	0.02	0.01	0.00
Para.	$k_{w,1}$	$k_{w,2}$	$k_{w,3}$	$k_{w,4}$	$k_{w,5}$
Value	0.001	0.001	0.001	0.001	0.001

TAB 4. parameter for control algorithm

The index 1, 2, 3 are for the three ovens, index 4 is for the water heater and the index 5 is for the coffee maker.

The complete simulated load profile is shown in Figure 9 (a) and (b).

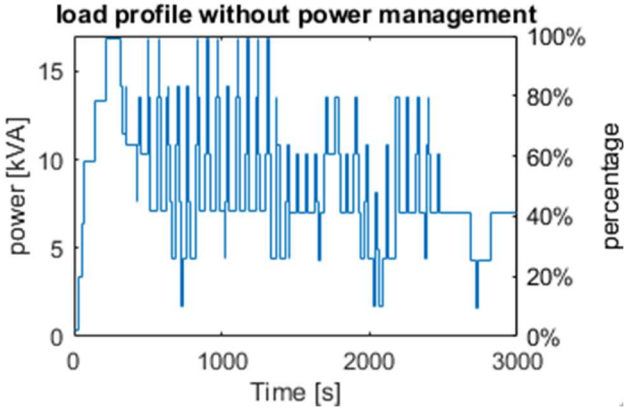


FIG 9. (a) load profile without power management

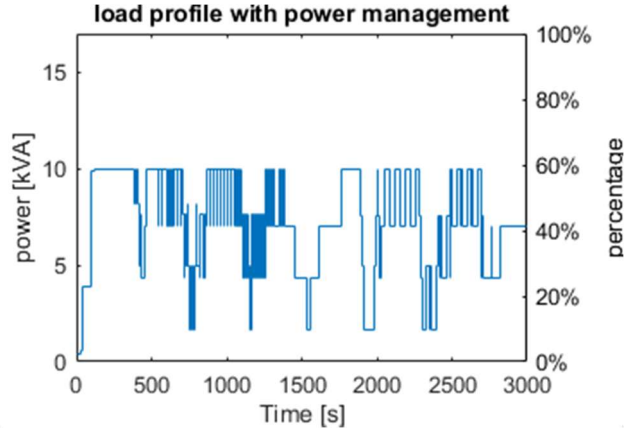


FIG 9. (b) load profile with power management

Figure 9 (a) illustrates the not managed load profile, where concurrent GAIN operation generates stochastic and repeated load switching with individual power spikes reaching 100% (*i.e.*,16.60 kVA) of total installed capacity. In contrast, Figure 9 (b) displays the load profile controlled by the adaptive power management system, which strictly caps aggregate power consumption at a 60% (*i.e.,* 9.96 kVA) level. While the managed profile successfully eliminates severe power spikes and flattens power consumption through dynamic load shedding and duty cycling.

5. RESULTS

As shown in Figure 10 the aggregate load profiles confirm the efficacy of the proposed adaptive priority-based load management algorithm (*cf.* “to be”). Under not managed conditions, simultaneous equipment operation induces a pronounced peak demand reaching up to 100% of installed capacity (*cf.* “as is”). Enforcing the target load management factor of 0.60 successfully restricts peak aggregated power consumption to 60%, achieving a 40% reduction in peak load spikes. However, capping peak demand inherently redistributes deferred work over a longer operational window. Consequently, the total process execution time for a complete catering cycle extends by approximately 30% (*cf.* Figure 10: meal service cycle “as is” *vs.* “to be”). This temporal expansion is effectively governed by the starvation prevention mechanism, ensuring all thermal and service constraints are met without violating power limits.

CC BY 4.0

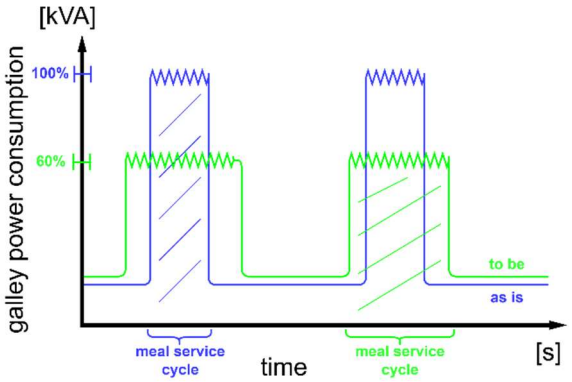


FIG 10. reduction of peak electrical power consumption during catering process

By implementing active power management to cap aggregate peak demand at 60%, the maximum continuous current requirement for the primary power supply line is significantly reduced. It is expected, that this reduction in current allows the main feeder lines to be downsized from AWG 2 to AWG 4 while maintaining compliance with standard voltage drop and current carrying capacity limits. Because AWG 4 conductors have a smaller cross-sectional area and lower linear density than AWG 2 cables, transitioning to the thinner gauge reduces the total mass of the power transmission cables by approximately 38%, *i.e.,* 60 kg for wiring [14]. A non-published estimation of electrical generator specific mass per kVA points to a weight saving of 20%, *i.e.,* approx. 20 kg, and 25 kVA per generator. Downsizing the feeder lines and generators directly cut off the overall mass of the electrical system, contributing directly to aircraft weight savings and improved fuel efficiency.

6. CONCLUSION AND OUTLOOK

Conventional aircraft power system architectures typically employ a top-down design methodology, where power budgets are assigned down to sub-systems based on worst-case concurrent sum assumptions. In contrast, this work adopts a bottom-up approach. By modeling the fundamental physical processes within the galley, specifically the thermal behavior of ovens, working cycle durations of beverage equipment, and realistic human service timelines, the system achieves demand reduction at the source. Understanding appliance dynamics at the process level enables intelligent load management without requiring operational restrictions on cabin crew.

A central outcome of this simulation-based research is the successful reduction of peak electrical power demand within the galley network from 100% to the target threshold of 60% without compromising catering service schedule or quality of service. This different from conventional aircraft design practices, which rely on top-down power allocation based on the worst-case concurrent sum of all installed appliances. Our work innovatively proposes a bottom-up load management framework to address demand dynamics in the process. Capping aggregate peak demand by 40% at the source yields significant system level benefits for the broader aircraft electrical power system. Controlling peak power demand enables the downsizing of electrical feeders, circuit breakers, and controllers.

The current work has laid the foundation for future research. The developed model and simulation environment are structured modularly. They can be used for other aircraft and galley configurations with simple modification of GAINs. Our bottom-up control strategy in the galley offers strong potential for integration into next-generation High Voltage Direct Current (HVDC) power architectures. The introduction of HVDC offers several benefits, most prominently, making the feedback control possible.

ACKNOWLEDGEMENTS

This work was supported by the LuFo VI-3 project “Galley Efficiency Catering Operations” (GECO, project number 20K2204E) funded by the Federal Ministry for Economic Affairs and Climate Action based on the decision of the German Bundestag.

Contact address:

lang.yu@tuhh.de

REFERENCES

[1] D. Schlabe, D, Zimmer, A. Pollok. *Exploitation strategies of cabin and galley thermal dynamics*, 2017 AeroTech Congress & Exhibition, Sep. 2017. https://saemobilus.sae.org/papers/exploitation-strategies-cabin-galley-thermal-dynamics-2017-01-2037 (accessed 2026/04/09)

[2] T. Schröter. *Power management on aircraft*. Dissertation, 2021

[3] D. Schlabe, J. Lienig. *Energy management of aircraft electrical systems-state of the art and further directions*. In Electrical Systems for Aircraft, Railway and Ship Propulsion, 1-6, 2012. https://ieeexplore.ieee.org/abstract/document/6387387 (accessed 2026/04/09)

[4] Unpublished results; *cf.* Concert Steam and Convection Oven, SAFRAN Cabin Inc, https://www.safran-group.com/products-services/concert-steam-and-convection-oven-new-ergonomic-and-robust-features-best-served-meals (accessed 2026/04/09)

[5] A. P. Ramallo-González, M. E. Eames, D. A. Coley. *Lumped parameter models for building thermal modelling: An analytic approach to simplifying complex multi-layered constructions*. Energy and Buildings, 60, 174-184, 2013. https://www.sciencedirect.com/science/article/pii/S0378778813000315 (accessed 2026/04/09)

[6] E. Ramírez-Laboreo, C. Sags, S. Llorente. *Thermal modeling, analysis and control using an electrical analogy* in 22nd Mediterranean Conference on Control and Automation, pp. 505-510, IEEE, 2014. https://ieeexplore.ieee.org/abstract/document/6961423 (accessed 2026/04/09)

[7] A. Shabani, D. Dhamo, D. Panxhi, O. Zavalani. *Modelling and simulation of home appliances using electric circuit analogy: Albanian case study*. In 2019 IEEE PES Innovative Smart Grid Technologies Europe (ISGT-Europe), pp. 1-5, IEEE, 2019.

[8] Turkish airlines Boeing 777-300ER V.2 Seat maps, Turkish Airlines, https://www.turkishairlines.com/de-int/flights/fly-different/fleet/boeing-777-300-er/ (accessed 2026/04/09)

CC BY 4.0

[9] Hazard Analysis and Critical Control Point (HACCP) System and Guidelines for Its Application, Annex to CAC/RCP 1-1969, Codex Alimentarius Commission, World Health Organization, Food and Agriculture Organization of the United Nations, 2020.

[10] MATLAB/Simulink version R2024b. Natick, Massachusetts: The MathWorks Inc.; 2016.

[11] P. J. Linstrom and W. G. Mallard, Eds., *NIST Chemistry WebBook, NIST Standard Reference Database Number 69*, National Institute of Standards and Technology, Gaithersburg, MD, 20899. doi: 10.18434/T4D303. 2026.

[12] Aeronautical Radio, Inc., "Definition of Standard Interfaces for Galley Insert (GAIN) Equipment, Physical Interfaces," ARINC Specification 810, SAE ITC, Annapolis, MD, 2021.

[13] J. Chen, K. Pitchai, S. Birla, R. Gonzalez, D. Jones, J. Subbiah. *Temperature-dependent dielectric and thermal properties of whey protein gel and mashed potato*. Transactions of the ASABE, 56(6), pp. 1457-1457, 2013. https://elibrary.asabe.org/abstract.asp-?aid=44130 (accessed 2026/04/09)

[14] Aerospace series - Cables, electrical for general purpose - Operating temperatures between -55 °C and 260 °C - Part 003: Product standard; German and English version EN 2854-003:2021 https://www.din-media.de/de/norm/din-en-2854-003/341079221 (accessed 2026/04/09)

CC BY 4.0